IEEE Photonics Journal
An IEEE Photonics Society Publication

Nanoholes Grating Couplers for Coupling Between Silicon-on-Insulator Waveguides and Optical Fibers

Volume 1, Number 3, September 2009

Xia Chen, Student Member, IEEE
Hon Ki Tsang, Senior Member, IEEE

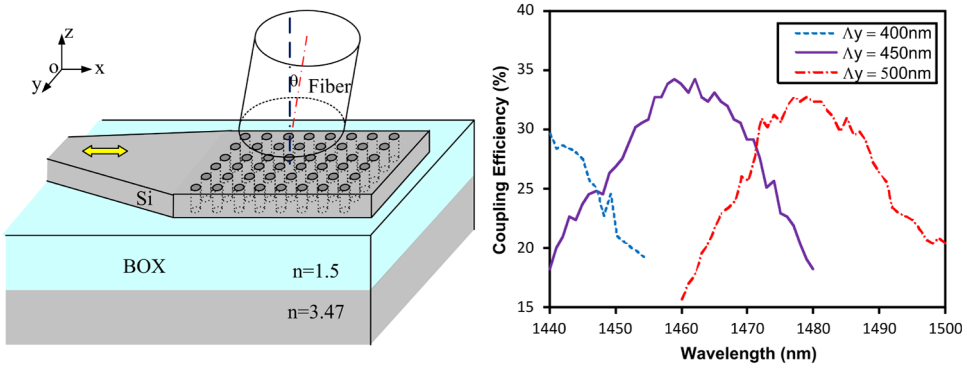

DOI: 10.1109/JPHOT.2009.2031685
1943-0655/$26.00 ©2009 IEEE

Nanoholes Grating Couplers for Coupling Between Silicon-on-Insulator Waveguides and Optical Fibers

Xia Chen, *Student Member, IEEE*, and Hon Ki Tsang, *Senior Member, IEEE*

Department of Electronic Engineering, The Chinese University of Hong Kong, Shatin, Hong Kong

DOI: 10.1109/JPHOT.2009.2031685
1943-0655/$26.00 ©2009 IEEE

Manuscript received August 3, 2009; revised August 27, 2009. First published Online August 31, 2009. Current version published September 18, 2009. This work was supported in part by the University Grants Committee of Hong Kong Special Administrative Region, China, under special equipment Grant CUHK-SEG01 and CUHK direct Grant 2050431. Corresponding author: H. K. Tsang (e-mail: hktsang@ee.cuhk.edu.hk).

Abstract: Simulation and experimental results of grating couplers composed of arrays of nanoholes are presented. The use of an array of holes instead of a conventional waveguide grating provides an additional degree of freedom in the design of the coupler, thus enabling fabrication using the same photolithography mask and etching process as used for the silicon-on-insulator (SOI) waveguides. A grating coupler with coupling efficiency as high as 34% for coupling between the TE mode of the silicon nanophotonic wire waveguide and a single-mode optical fiber and with 3-dB bandwidth of 40 nm was fabricated. A theoretical model is presented, and 3-D finite-difference time-domain simulations are used to optimize the coupler design.

Index Terms: Silicon nanophotonics, nanostructures, gratings, waveguides.

1. Introduction

Silicon-on-insulator (SOI) is a promising platform for a planar lightwave circuit (PLC) due to its high refractive index contrast and compatibility with the mature fabrication facilities for complementary metal–oxide–semiconductor (CMOS) technology. Various kinds of devices on SOI wafers have been demonstrated in recent years using nanophotonic wire waveguides which have cross-sectional dimensions of only a few hundred nanometers. The large coupling loss from the mode mismatch between optical fibers and the nanophotonic wires is one important problem that must be solved before silicon can replace silica as a mainstream platform for PLCs. Recently, waveguide grating couplers defined by shallow-etched grooves [1]–[3], metallic lines [4], and slanted grooves [5] have been used for efficient coupling to optical fibers. They have many advantages over alternative approaches that use adiabatic tapers and polished facets [6], including freedom for placement anywhere on a chip, avoiding need for facet polishing, enabling wafer-scale optical testing and potentially facilitating low-cost packaging. Grating couplers also offer such additional functionality as polarization or power splitters [7]–[9].

For those grating couplers mentioned previously, the lithography and etching processes needed to fabricate the grating structures must be distinct from the corresponding waveguide fabrication steps because of the different etch depths required for the grating couplers. Applying grating couplers that could be made with the same fabrication steps as used for the waveguides will reduce the total number of fabrication steps and the cost of the PLC. However, for conventional gratings formed by continuous lines which are etched to the depths typically needed for waveguide

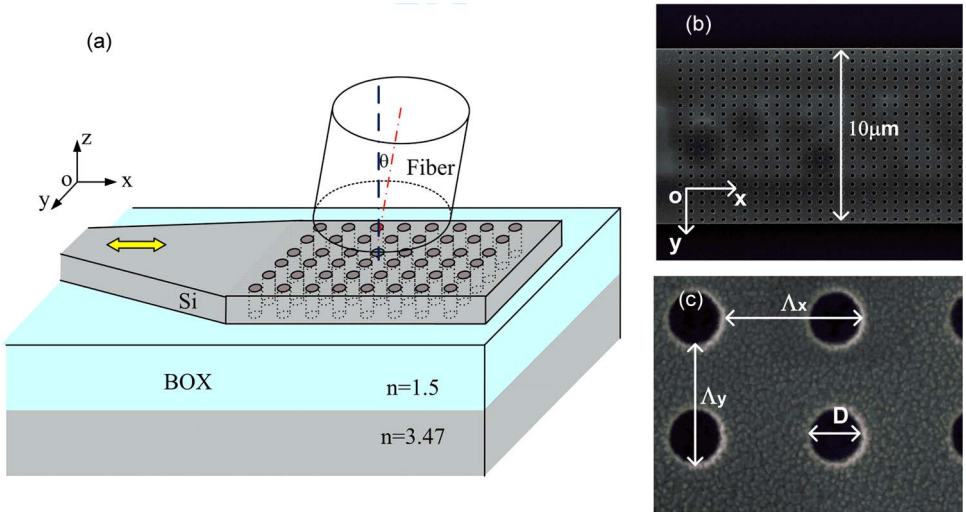

Fig. 1. (a) Schematic picture of the grating coupler for coupling between fibers and nanophotonic wire waveguides on SOI, $\theta = 8^{\circ}$. (b) Scanning electron microscope (SEM) image of the fabricated array of nanoholes on the 10-μm-width waveguide. The silicon dioxide on top was removed. (c) Nanoholes array with the holes diameter *D*, grating period Λ_x, and transversal holes period Λ_y defined (D = 200 nm, $\Lambda_x = 610$ nm, and $\Lambda_y = 500$ nm).

fabrication (to the buried oxide of the SOI wafer), the refractive index step introduced would normally be too large. For example, almost 50% of the light coming from the waveguide would be reflected by the first period. The grating strength in this case would be too strong for efficient coupling of light between waveguides and optical fibers. Subwavelength structures may be used to reduce the effective index step without distortion of the phase front of waveguide mode [10]. A single-etch grating coupler which could be fabricated by the same etch step as the waveguides, was recently proposed for coupling into the TM mode of the waveguide using subwavelength microstructures, and 3-D finite-difference time-domain (3-D FDTD) simulation results were reported in [11], but no devices were fabricated.

In this paper, we present both the simulation and experimental characterization results of a single-etch grating coupler formed by an array of nanoholes for coupling into the TE mode of the SOI waveguide as shown in Fig. 1. Nanoholes have less stringent photolithography requirements than the square-shaped microstructure proposed in [11] and can be produced using the standard deep-UV photolithography commonly used for CMOS devices. The coupling efficiency attained using the array of nanoholes (34% for TE polarization) is comparable with those obtained with other grating couplers [2]–[4], which were fabricated using additional photolithography and shallow etch steps. In this paper, we also describe a 2-D model for the proposed nanoholes grating coupler.

2. Two-Dimensional Model for Nanoholes Grating Couplers

Fig. 1(a) shows the schematic of the proposed single-etch nanoholes grating coupler. The device was fabricated using deep-UV photolithography (193 nm) on a SOI wafer, which has a 220-nm-thick top silicon layer (device layer) and 2000-nm-thick buried oxide layer. A 750-nm-thick oxide layer was deposited on top after fabrication of nanoholes array. This silicon dioxide layer can provide protection of devices and also slightly increase the percentage of light coupled upward [2]. The waveguides and grating couplers were formed together by dry etching to the buried oxide. Fig. 1(b) and (c) are the SEM images of the fabricated nanoholes grating coupler taken with the top oxide removed. Fig. 1(c) is a close-up view of the nanoholes array and the holes diameter *D*, grating period Λ_x, and transversal holes period Λ_y are defined as indicated in the figure. The hole diameter *D* was chosen to be 200 nm in the device design. A smaller hole diameter would give smaller back

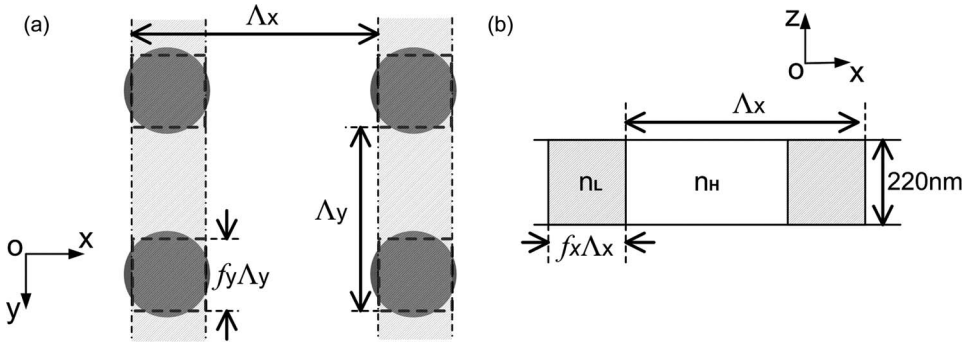

Fig. 2. (a) Top view of the nanohole array. Square-shaped holes with same area were used in calculation. First-order EMT was then applied to estimate the effective refractive index of the shaded region with nanoholes. (b) Two-dimensional model of the waveguide grating with nanoholes array based on a slab structure.

reflection into waveguide, but 200 nm was the minimum value that could be guaranteed by the fabrication technology. A single-mode optical fiber with 10.4-μm mode field diameter (MFD) was used for the input and output coupling. Following the approach used in conventional grating coupler designs [2], the coupling fiber is oriented at an angle of 8° off vertical in the x–z plane defined by the surface normal (*z*-axis) of SOI wafer and the waveguide direction (*x*-axis) in order to minimize second order Bragg reflection, which would otherwise limit the performance of the grating coupler as shown in Fig. 1(a). The width of the planar waveguide of the grating region was designed to be 10 μm, in order to have a good match with the MFD from the optical fiber laterally (in *y*-axis). The grating period could be calculated using the phase matching condition [9], [12]

$$q\lambda = \Lambda_x\left(n_{\text{eff}} - n_{\text{cladding}}\sin(\theta)\right). \tag{1}$$

In (1), λ is the center wavelength; n_{eff} is the effective index of the grating region with nanoholes array; θ is the off-vertical tilt angle of the fiber $(\theta = 8^\circ)$; n_{cladding} is the refractive index of the cladding material $(n_{\text{cladding}} = 1.5)$; q is the diffraction order (set equal to 1 for the first-order diffraction); and Λ_x is the grating period in the beam propagating direction.

We initially used (1) to estimate the grating period Λ_x. The average effective index of the nanoholes grating region could be calculated using a 2-D model based on a slab structure shown in Fig. 2(b). The section with higher index is made of 220-nm-thick silicon slab with refractive index of 3.47 and a cladding refractive index of 1.5. The effective index n_H for the fundamental mode was calculated to be 2.89 for wavelength of 1450 nm. The sections with lower index are made from silicon with nanoholes that are filled with cladding material (silicon dioxide) as shown in Fig. 2(a). The refractive indices are 3.47 and 1.5 for silicon and nanoholes, respectively.

For ease of calculation, we use square-shaped holes to represent the 200-nm-diameter round-shaped holes. The side length of the square-shaped holes is set to be 177 nm in order to have the same area as the round-shaped holes. Similar to the subwavelength structure in [10], the first-order effective medium theory (EMT) [13] could be used to estimate the effective refractive index of the shaded region in Fig. 2(a). According to EMT, a composite medium comprising two different materials interleaved at the subwavelength scale can be approximated as a homogenous medium. The first-order expressions for anisotropic refractive index are given by

$$n^{\text{TM}} = \left[f_y n_{\text{hole}}^2 + (1 - f_y) n_{\text{Si}}^2\right]^{1/2} \tag{2a}$$

$$\frac{1}{n^{\text{TE}}} = \left[\frac{f_y}{n_{\text{hole}}^2} + \frac{(1 - f_y)}{n_{\text{Si}}^2}\right]^{1/2} \tag{2b}$$

where the symbol n_{hole} is the refractive index of the nanoholes (equal to 1.5), and n_{Si} is the refractive index of silicon slab (equal to 3.47). By assuming the transversal holes period Λ_y equals

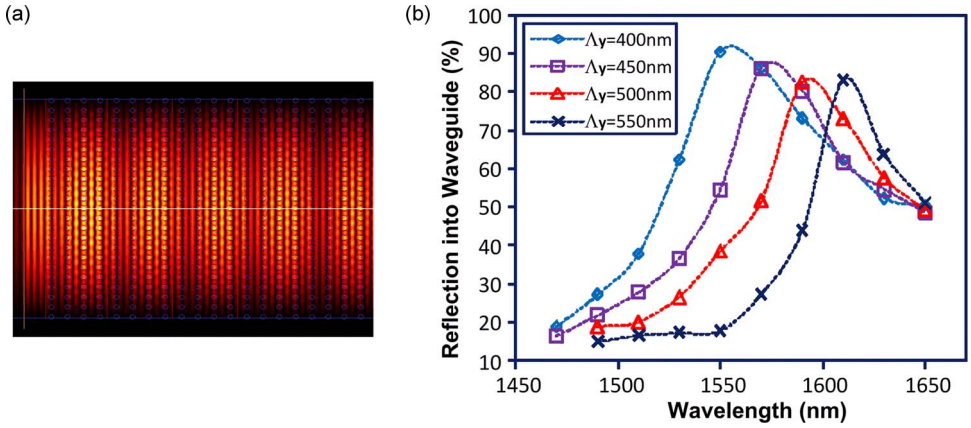

Fig. 3. (a) Color-graded representation of the mode field amplitudes in the grating region obtained from 3-D FDTD simulation of the nanoholes grating coupler with $\lambda = 1490$, $\Lambda_y = 450$, $\Lambda_x = 610$, and $D = 200$ nm. (b) Simulation results of the back reflection into waveguide from the nanoholes grating ($D = 200$ and $\Lambda_x = 610$ nm) as a function of wavelength for Λ_y between 400 and 550 nm. The wavelength of the second-order Bragg reflection shifts with change of Λ_y.

500 nm, transversal fill factor of nanoholes f_y would be equal to 0.35. In our geometry, the electric field of the TE mode of waveguide is perpendicular to the nanoholes. Equation (2b) should be used to calculated the refractive index of the shaded region, which equals to 2.18. The effective refractive index for the fundamental mode of the slab in the shaded region is then calculated, and in this case, it is equal to 1.76.

For the fundamental mode in the grating structure shown in Fig. 2(b), the average effective index of the grating region n_{eff} for the fundamental mode was obtained using

$$n_{\text{eff}} = f_x n_L + (1 - f_x) n_H. \tag{3}$$

Thus, the value of n_{eff} is about 2.6 for grating structure with $\Lambda_y = 500$ nm and $\Lambda_x = 610$ nm. The center wavelength of light coupling is 1450 nm for a grating period of 610 nm based on (1).

3. Three-Dimensional FDTD Simulation and Measurement Results

The 2-D model mentioned in Section 2 requires the transversal holes period Λ_y to be as small as possible compared to the effective wavelength in the medium. A more precise result would be obtained using 3-D FDTD simulations. The results of the 3-D FDTD simulations, such as shown in Fig. 3(a), allowed the transversal period Λ_y of the nanoholes to be varied and the coupler design for the desired wavelength to be optimized. The fundamental waveguide mode was calculated and propagated into the grating region containing the nanoholes array $(\text{D} = 200\ \text{nm})$. The percentage of power reflected back from grating into waveguide for different transversal period Λ_y of the nanoholes and different wavelengths was calculated and plotted in Fig. 3(b). The wavelength of peak reflection varied with the transversal period Λ_y, as shown in the figure.

The peak reflection occurs at the wavelength of second order Bragg back reflection (phase matching condition). The wavelength of peak reflection could also be determined by the simple equation $\lambda_{\text{p}} = \Lambda_x \times n_{\text{eff}}$ [2]. Using this equation, we calculated the effective index of the grating region with nanoholes array. We found that the effective index obtained from the 3-D FDTD simulations varied almost linearly from 2.64 to 2.55 with the transversal period Λ_y, which was varied from 550 nm to 400 nm. From (1), the center wavelength for coupling with $\theta = 8^\circ$ may be calculated and this is plotted in Fig. 4 together with the experimental data. The center wavelength calculated using the 2-D model described in Section 2 is also plotted in the same figure. We can see that the results obtained by 3-D FDTD simulations are smaller than the experimental data. This is because the refractive index will increase slightly when the wavelength was reduced (from around 1560 nm

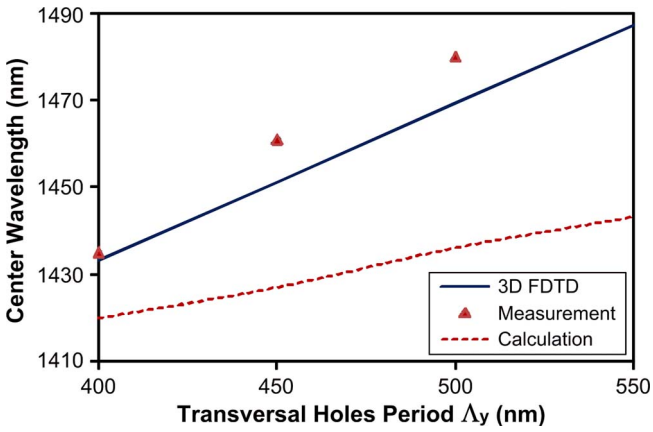

Fig. 4. Center wavelength of the nanohole grating coupler with $\theta = 8^\circ$ was calculated based on 3-D FDTD simulations for different transversal hole period Λ_y. The experimentally measured data and calculated result by the 2-D model described in Section 2 are also presented.

to around 1450 nm). Higher effective refractive index will lead to longer center wavelength. We can also observe that the result obtained by the proposed 2-D model would become more and more inaccurate with the increasing of transversal period Λ_y, as the EMT used in the model requires the transversal period Λ_y as small as possible compare to the wavelength in the medium [10], [13].

From Fig. 3(b), it can be seen that as the transversal period Λ_y is reduced, the bandwidth of reflection increases, and the back reflection at the coupling wavelength would also increase. This bandwidth of reflection would become even larger for the fabricated devices when incorporated with the fabrication errors. We measured the Fabry–Perot (FP) resonances around the center wavelength for different nanoholes grating couplers. Strong FP resonances (3.8-dB peak to trough extinction ratio) with about 0.1-nm free spectral range (FSR) were observed for the grating coupler with $\Lambda_y = 400$ nm. This extinction ratio was reduced to 1.6 dB and 0.8 dB for 450-nm and 500-nm transversal period, respectively. Using the well-known expression for FP FSR $\Delta\lambda \approx \lambda_o^2/2n_gL$, for a cavity length L (equal to 3 mm for the fabricated devices), and the calculated average group index $n_g \approx 4$ at wavelength around 1460 nm, the calculated FSR is about 0.09 nm. This agrees with the measurements and confirms that spectral oscillations are from FP resonances formed by the reflections between the grating couplers at each end of the waveguide. The large back reflection for grating coupler with $\Lambda_y = 400$ nm leads to a lower coupling efficiency.

We characterized the fabricated nanoholes grating coupler by measuring the fiber-waveguide-fiber insertion loss of light coupled via a pair of grating couplers separated by a 500-nm-wide waveguide of 2-mm length. The grating with nanoholes array in x-direction would diffract light into/from a cleaved single-mode optical fiber with 8° tilt. Two 0.5-mm-long adiabatic tapers were used to connect the input and output 10-μm-wide waveguide with the 500-nm-wide nanophotonic waveguide. Assuming that the coupling efficiencies were the same for the couplers at both ends and neglecting the waveguide propagation losses, the coupling efficiency was obtained for different transversal holes period Λ_y and plotted in Fig. 5. With $\Lambda_y = 450$ nm, we obtained 34% coupling efficiency at 1460 nm with a 3-dB bandwidth of 40 nm. Limited by the wavelength range of our tunable laser, we could only measure the coupling efficiency down to 1440-nm wavelength. The center wavelength of the coupler with $\Lambda_y = 400$ nm was obtained by curve fitting. The center wavelengths of the fabricated couplers were 1435 nm, 1461 nm and 1480 nm for 400-nm, 450-nm and 500-nm transversal period Λ_y, respectively as shown in Fig. 5. The coupling efficiency was mainly limited by the bidirectional nature of diffraction. Adding a substrate mirror would further improve the performance. 69% coupling efficiency to slightly tilted optical fiber was measured in [14] for a shallow-etched grating coupler with a metal bottom mirror. We expect this order of coupling efficiency to be attainable for the nanohole grating coupler design.

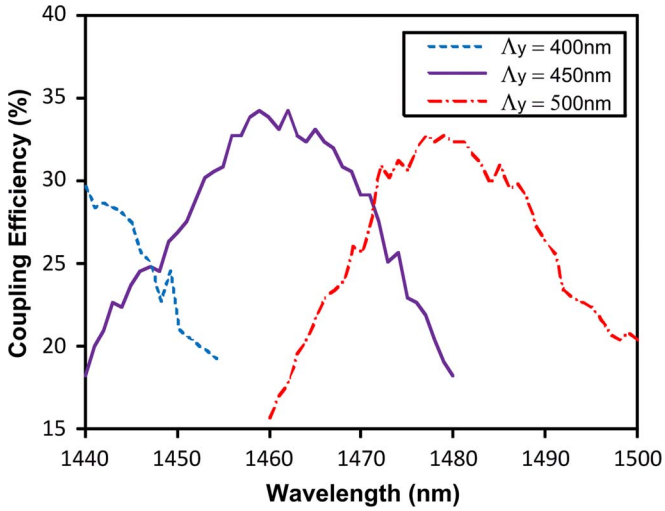

Fig. 5. Experimentally measured coupling efficiencies were plotted for the proposed nanohole grating couplers with different transversal period Λ_y. Thirty four percent peak coupling efficiency was measured for $\Lambda_y = 450$ nm.

4. Conclusion

In summary, grating couplers formed by an array of nanoholes was proposed, fabricated, and experimentally characterized. The grating couplers were fabricated in the same deep-etch step as used for defining the waveguides, thus reducing the number of masks and fabrication steps needed. Despite the reduction in fabrication steps, we achieved coupling efficiencies comparable with conventional grating couplers that use additional fabrication processes. The 34% coupling efficiency measured in the fabricated devices had a 40-nm, 3-dB optical bandwidth for coupling between single-mode optical fibers and the silicon nanophotonic wire waveguides. The 3-D FDTD simulation results had good agreement with the experimental results from the fabricated devices. Further improvement could be achieved by varying the grating strength to increase the field overlap with fiber mode [11] and adding a substrate mirror [14].

Acknowledgment

The authors thank ePIXfab (www.epixfab.eu) for the fabrication of the devices made with deep UV photolithography.

References

[1] D. Taillaert, W. Bogaerts, P. Bienstman, T. F. Krauss, P. Van Daele, I. Moerman, S. Verstuyft, K. De Mesel, and R. Baets, "An out-of-plane grating coupler for efficient butt-coupling between compact planar waveguides and single-mode fibers," *IEEE J. Quantum Electron.*, vol. 38, no. 7, pp. 949–955, Jul. 2002.

[2] D. Taillaert, F. Van Laere, M. Ayre, W. Bogaerts, D. Van Thourhout, P. Bienstman, and R. Baets, "Grating couplers for coupling between optical fibers and nanophotonic waveguides," *Jpn. J. Appl. Phys.*, vol. 45, no. 8A, pp. 6071–6077, Aug. 2006.

[3] X. Chen, C. Li, and H. K. Tsang, "Fabrication-tolerant waveguide chirped grating coupler for coupling to a perfectly vertical optical fiber," *IEEE Photon. Technol. Lett.*, vol. 20, no. 23, pp. 1914–1916, Dec. 2008.

[4] S. Scheerlinck, J. Schrauwen, F. Van Laere, D. Taillaert, D. Van Thourhout, and R. Baets, "Efficient, broadband and compact metal grating couplers for silicon-on-insulator waveguides," *Opt. Express*, vol. 15, no. 15, pp. 9625–9630, Jul. 2007.

[5] B. Wang, J. H. Jiang, and G. P. Nordin, "Embedded slanted grating for vertical coupling between fibers and silicon-on-insulator planar waveguides," *IEEE Photon. Technol. Lett.*, vol. 17, no. 9, pp. 1884–1886, Sep. 2005.

[6] T. Shoji, T. Tsuchizawa, T. Watanabe, K. Yamada, and H. Morita, "Low loss mode size converter from 0.3 μm^2 Si wire waveguides to single-mode fibers," *Electron. Lett.*, vol. 38, no. 25, pp. 1669–1670, Dec. 2002.

[7] D. Taillaert, H. Chong, P. I. Borel, L. H. Frandsen, R. M. De La Rue, and R. Baets, "A compact two-dimensional grating coupler used as a polarization splitter," *IEEE Photon. Technol. Lett.*, vol. 15, no. 9, pp. 1249–1251, Sep. 2003.

[8] X. Chen, C. Li, and H. K. Tsang, "Etched waveguide grating variable 1 × 2 splitter/combiner and waveguide coupler," *IEEE Photon. Technol. Lett.*, vol. 21, no. 5, pp. 268–270, Mar. 2009.
[9] Y. B. Tang, D. X. Dai, and S. L. He, "Proposal for a grating waveguide serving as both a polarization splitter and an efficient coupler for silicon-on-insulator nanophotonic circuits," *IEEE Photon. Technol. Lett.*, vol. 21, no. 4, pp. 242–244, Feb. 2009.
[10] J. H. Schmid, P. Cheben, S. Janz, J. Lapointe, E. Post, and D. X. Xu, "Gradient-index antireflective subwavelength structures for planar waveguide facets," *Opt. Lett.*, vol. 32, no. 13, pp. 1794–1796, Jul. 2007.
[11] R. Halir, P. Cheben, S. Janz, D. X. Xu, I. Molina-Fernandez, and J. G. Wanguemert-Perez, "Waveguide grating coupler with subwavelength microstructures," *Opt. Lett.*, vol. 34, no. 9, pp. 1408–1410, May 2009.
[12] R. Orobtchouk, A. Layadi, H. Gualous, D. Pascal, A. Koster, and S. Laval, "High-efficiency light coupling in a submicrometric silicon-on-insulator waveguide," *Appl. Opt.*, vol. 39, no. 31, pp. 5773–5777, Nov. 2000.
[13] S. M. Rytov, "Electromagnetic properties of a finely stratified medium," *Sov. Phys. JETP*, vol. 2, no. 3, pp. 466–475, 1956.
[14] F. Van Laere, G. Roelkens, M. Ayre, J. Schrauwen, D. Taillaert, D. Van Thourhout, T. E. Krauss, and R. Baets, "Compact and highly efficient grating couplers between optical fiber and nanophotonic waveguides," *J. Lightwave Technol.*, vol. 25, no. 1, pp. 151–156, Jan. 2007.